Dynamics of a Sonoluminescing Bubble in Sulfuric Acid

Stephen D. Hopkins,[1] Seth J. Putterman,[2,3] Brian A. Kappus,[2] Kenneth S. Suslick,[1] and Carlos G. Camara[2]

[1]*Department of Chemistry, University of Illinois at Urbana-Champaign, Urbana, Illinois 61801, USA*

[2]*Physics Department, University of California, Los Angeles, California 90095, USA*

[3]*California Nano-Systems Institute, University of California, Los Angeles, California 90095, USA*

(Received 19 May 2005; published 14 December 2005)

The spectral shape and observed sonoluminescence emission from Xe bubbles in concentrated sulfuric acid is consistent only with blackbody emission from a spherical surface that fills the bubble. The interior of the observed 7000 K blackbody must be at least 4 times hotter than the emitting surface in order that the equilibrium light-matter interaction length be smaller than the radius. Bright emission is correlated with long emission times (~ 10 ns), sharp thresholds, unstable translational motion, and implosions that are sufficiently weak that contributions from the van der Waals hard core are small.

DOI: 10.1103/PhysRevLett.95.254301 PACS numbers: 78.60.Mq

Sonoluminescence (SL) is an excellent example of an energy focusing phenomenon. The interaction between a diffuse sound wave and a small isolated bubble concentrates vibrational energy by 12 orders of magnitude to create flashes of UV light [1]. In water, the spectrum of single bubble sonoluminescence matches, within experimental error, blackbody radiation with surface temperatures in the range 6000–20 000 K [2] for sound frequencies between 10 and 50 kHz. At 1 MHz the spectrum matches thermal bremsstrahlung from a 10^6 K plasma [3]. As SL originates from highly compressed gas inside a pulsating bubble, attempts to increase the efficiency of cavitation have considered the role of the vapor of the surrounding fluid [4–9]. High vapor pressure and complex molecules (e.g., acetone) would in this view cushion the collapse and soak up the compressive heating [10], whereas low vapor pressure fluids with noble gas bubbles would optimize the concentration of the energy density. From this perspective sulfuric acid (with a vapor pressure less than 1% that of water) is an excellent candidate for substantially improving the efficiency of SL [11,12]. At 30 kHz, the sulfuric acid system also permits single bubble sonoluminescence [11] comprised of flashes that can be 2700 times brighter [12] than the standard room temperature argon bubble in water. In the water hammer realization of SL [13], use of low vapor pressure fluids, e.g., phosphoric acid yields an upscaling of standard SL flashes by 7 orders of magnitude to yield 10^{12} photons/flash [14].

We report here that the sulfuric acid noble gas system is unique in single bubble sonoluminescence in its extreme sensitivity to dissolved gas concentration in the fluid. Furthermore, the dramatically increased brightness is accompanied by instability in the bubble dynamics. The instability is manifested through quickly translating bubbles whose implosion parameters such as maximum radius and implosion velocity vary from one sound cycle to the next. Only on those cycles where the collapse velocity exceeds a sharp threshold is light emitted. Although these experiments were motivated by arguments suggesting that low vapor pressure upscales SL, conclusions relating to the role of vapor pressure are complicated by our observation that for fluid-gas mixtures which minimize the jittery translational motion, SL in water and SL in sulfuric acid are very similar phenomena with the same light emission.

Experiments are carried out in an aqueous solution that is 85% sulfuric acid (SA) by weight. Xenon is mixed into the solution under pressure heads ranging from 4 to 50 torr, transferred to the resonator under vacuum and then opened to 1 atm. A bubble was seeded at the velocity node of the standing sound wave with a 100 mJ, 3 ns pulse of light from a Nd:YAG laser. Mie light scattering was used to measure the radius R of the bubble as a function of time t: $R(t)$ [15]. The data are matched to a simulation determined from solving the Rayleigh-Plesset equation coupled to thermal conduction [16] as set forth by Prosperetti [17] which allows for continuous transition from isothermal to adiabatic heating of the bubble interior. We find that for SA bubbles with 50 torr of xenon the interior is isothermal for $R > 2R_0$. We use the fits to determine the ambient radius R_0, the collapse radius R_c, the maximum radius R_m, and the effective driving pressure P_a of the imposed sound field (this effective P_a could differ substantially from the value extrapolated from hydrophone measurements in the noncavitating fluid). Spectra were acquired by an imaging spectrometer coupled to an intensified CCD [3] via a fiber optic element.

Figure 1 shows the spectrum of light from bubbles formed from a 4 torr solution of xenon in the SA. Even though the ambient vapor pressure of the SA (0.04 torr) is over 100 times less than water at 1 °C, the total light emission from these systems is almost identical. Furthermore, measurements of flash width in both cases are <500 ps and instrument limited. We have been unable to take spectra of SL from SA near 0 °C because of our inability to seed a single pulsating bubble.

The $R(t)$ for a single sonoluminescing bubble formed from a 4 torr solution of xenon in SA is shown in Fig. 2. The solid line is a fit to the data and the dotted and dashed

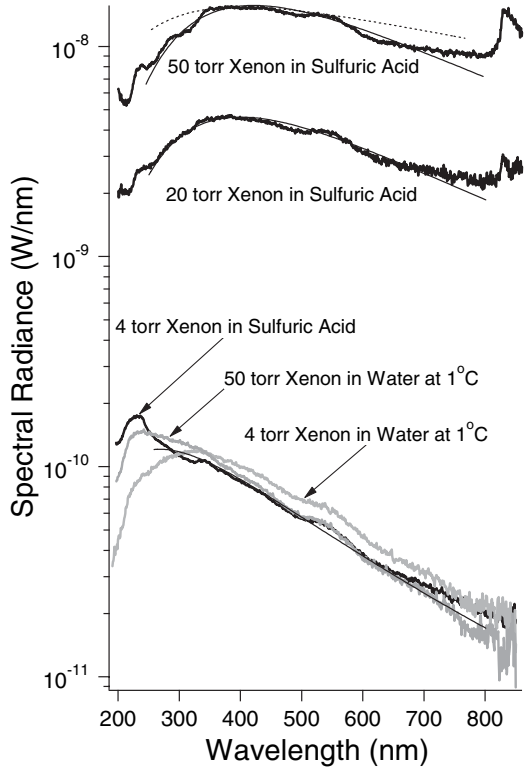

FIG. 1. Spectra of SL for bubbles formed from various concentrations of xenon in room temperature sulfuric acid, as compared with xenon bubbles in 1 °C water at maximum acoustic pressure before loss of bubbles. The 4 torr bubbles are very similar (with the 4 torr xenon in SA matching blackbody emission with a temperature of 10 000 K), whereas the 50 torr bubbles are dramatically different. The 50 torr SA bubbles emit over 5×10^8 photons/flash; its continuum is well fit by blackbody temperatures in the range 6800–7000 K (solid line through the 50 torr xenon in SA data). Also shown is the best fit bremsstrahlung (dotted line) that has been scaled up by a factor of 4 to match the 400 nm observed peak. Data are corrected for the extinction coefficient of the fiber but not for transmission through the SA or its container. Flash widths of <0.5 ns for the 4 torr bubble were measured with a photomultiplier tube (PMT) (Hamamatsu R2809U) with a rise time of 170 ps, through an oscilloscope with a rise time of 200 ps in single shot mode and were instrument limited. The 10 ns flash width for the 50 torr bubble was similarly measured using a (Hamamatsu H5783-03) PMT with a rise time of 650 ps. For this case, the shot to shot variation in flash width was about 30%.

lines are best fits to the $R(t)$ for a 4 torr xenon bubble in pure water. It can be seen that there is no significant experimental difference in the dynamical motion of these bubbles. The bubble in cold water achieves a 50% larger radius than the bubble in SA. This can be accounted for by the viscosity of SA which is 14 times larger than for pure water near 0 °C. For SA the viscosity is large enough to resist the expansion of the bubble during the rarefaction portion of the cycle. All of these bubbles have similar expansion ratios "R_m/R_0," which range from 7.3 (SA) to 9.3 (1 °C water).

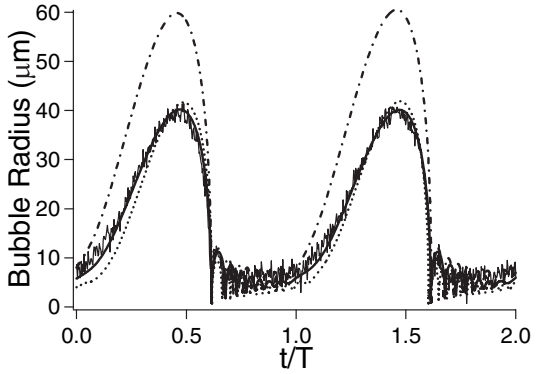

FIG. 2. Radius as a function of time for xenon bubbles formed from 4 torr solutions: SA (data and solid line), water (dotted line, room temperature; dashed line, 1 °C). Fit parameters are, respectively, $R_0 = 5.5, 4.5, 6.4$ μm; $P_a = 1.65, 1.5, 1.75$ atm. The calculated collapse radius (R_c) is 0.85 μm and the hard core radius (a) is 0.7 μm for the SA bubble. The period of the sound field is $T = 37.8$ kHz for SA, 39.5 kHz for water, and 39.7 kHz for 1 °C water). Fit parameters also include the SA density of 1.8×10^3 kg/m^3, speed of sound of 1.47×10^3 m/s, viscosity of 25 mPa · s, and a surface tension of 55 mN/m.

As the noble gas content of the fluid is increased the behavior of cavitation in water and SA diverge. Light emission from SA increases by about a factor of 100 (Fig. 1) and the flash width increases by over a factor of 10. This effect is accompanied by an increase in the ambient bubble radius by about a factor of 3, a decrease in the expansion ratio to about 3.5, and an increase in translational motion of the bubble. Figure 3 displays two different states of bubble motion that are representative of a variety of possible dynamics. It is important to note that switching between these states is spontaneous and uncontrolled. Changes in R_0 and P_a are not caused by changes in the drive applied (which is constant). The 50 torr bubble is representative of moving single bubble sonoluminescence [18] and the effective P_a acting on the bubble is affected by its motion [19] which can follow arcs as large as 1 cm. The $R(t)$ curve in Fig. 3(a) indicates a bubble with an ambient radius of 15 μm, which emits light every other cycle. The fit parameters remain fixed throughout the 4 plotted collapses, indicating that Rayleigh's equation mimics the observed alternating pattern in the acquired data. In Fig. 3(b) $R_0 = 16$ μm, and this bubble emits light every period, with each flash being about 10 times brighter than the alternating SL bubble state of Fig. 3(a). Good fits can be obtained for a $\pm 10\%$ change in P_a, which require a corresponding percentage change in R_0. The observed spectrum in Fig. 1 is an average over the entire range of motions. For larger xenon concentrations the bubbles become increasingly unstable. We were unable to trap single bubbles at or above 150 torr of Xe.

The maximum speed of collapse as calculated from the Rayleigh-Plesset fit to the data is a diagnostic of the

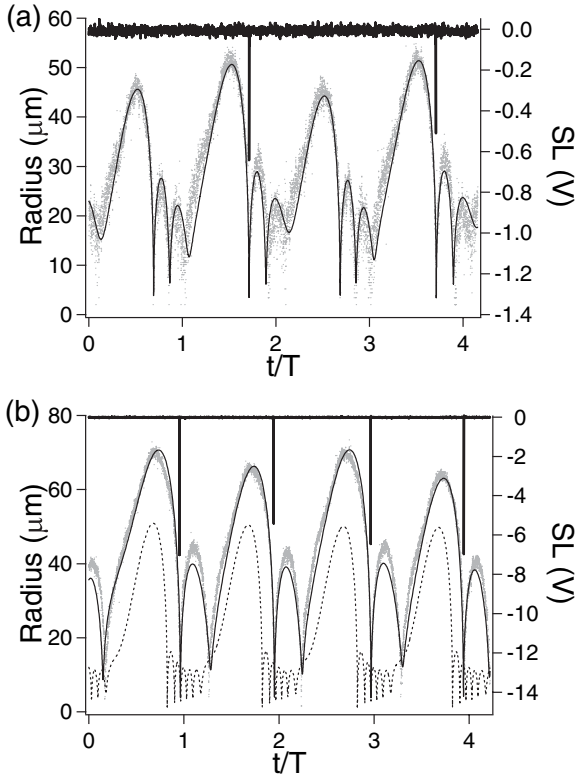

FIG. 3. Various $R(t)$ curves observed for bubbles formed from 50 torr mixtures of xenon in aqueous SA, showing timing and relative strength of SL. (a) $R_0 = 15$ μm, $P_a = 1.5$ atm; minimum radius 4.3 μm SL, 4.6 μm no SL; (b) $R_0 = 16$ μm, $P_a = 1.6$ atm, minimum radius near 4.1 μm for all collapses and the hard core radius is 2.5 μm. The dashed line displays a 50 torr xenon bubble in 1 °C water; $R_0 = 7.8$ μm, $P_a = 1.53$ atm. The right axis "SL (V)" gives the strength of the SL signal as measured by a Hamamatsu H5783-03 PMT and read out by the 50 Ω input on an Infinium Oscilloscope. The single photoelectron level is ~30 mV.

strength of a bubble implosion. For the fit in Fig. 3(a) the light-emitting cycles are characterized by a maximum collapse velocity greater than 120 m/s, whereas in the non-light-emitting cycles the maximum bubble velocity is less than 80 m/s. This 50% difference apparently accounts for the distinction between bright SL and no SL. The range of parameters that yield a good fit to these data extends to $R_0 \pm 1$ μm and $P_a \pm 0.1$ atm. For all cases the difference in velocity for SL and no SL is at least 20%. Perhaps, this threshold for SL is a clue to the nonlinear process (e.g., an imploding shock wave) [20–22] that concentrates energy inside the bubble and makes SL possible. In the lower panel of Fig. 3 the speed of collapse ranges between 210 and 260 m/s, which exceeds the ambient speed of sound of 170 m/s. In this case light is emitted on each cycle. For the 50 torr Xe bubble in water the ambient radius is smaller being 7.8 μm and the collapse velocity is much faster being 1400 m/s. This speed approaches the sound velocity in water and is clearly well outside the range of validity of Rayleigh's equation [23].

The calculated Bjerknes force acts on the light-emitting bubble so as to generate unstable translational motion and variations in bubble size. The smaller bubble shown in Fig. 3(a) has a net Bjerknes force directed towards the pressure antinode, while the larger bubble in Fig. 3(b) has a net Bjerknes force of the opposite sign [Ref. [15], Eq. (22)]. According to Fig. 1 the continuum contribution to the spectrum of the 50 torr xenon in aqueous SA has a blackbody temperature of ~7000 K. By combining Planck's law with the measured flash width of 10 ns one arrives at a value for the radius of the light-emitting surface: $R_e \sim 3.9$ μm. The size of the hot spot is therefore close to the calculated minimum radius ($R_c \sim 4.0$ μm) of the bubble's motion. Thermal bremsstrahlung from an equilibrium transparent plasma is another mechanism that generates a broadband spectrum [20,24]. The best fit bremsstrahlung spectrum has a temperature of 17 500 K. Even at this elevated temperature, the calculated bremsstrahlung intensity [as determined from the spectral emission coefficient (Ref. [24], Eq. 5.15) with a 3% ionization as derived from the Saha equation (Ref. [25], Eq. 9.11.11)] is lower by a factor of 4 than the intensity calculated for a 7000 K blackbody. In addition to this lower intensity, the shape of the bremsstrahlung curve does not fit the data as well as the blackbody curve. Adjustments to the temperature cause the shape of the bremsstrahlung fit to diverge even further from the data. The maximal efficiency of blackbody radiation appears to make it a compelling candidate for continuum emission from the SA bubbles described here (N.B., in this discussion, we have considered only sources with nonzero absorption coefficients at the observed wavelengths; e.g., atomic luminescence lines are separate from this analysis).

The bright SA spectrum also provides evidence for an inner core that is hotter than the measured emission. Even at 17 500 K the mean free path for light in compressed xenon (1.85×10^{21}/cc) is 250 μm (Ref. [24], Eq. 5.21), which is much bigger than R_e. In order to achieve an equilibrium mean free path smaller than R_e at 400 nm requires a temperature in excess of 3 eV.

Above ~800 nm the bubbles in SA show deviations from a blackbody spectrum due to the appearance of emission lines, which are a property of SL when bubbles have translational motion [12,16,26–28]. There has been success in identifying the relevant atomic and molecular transitions [12,18] and the spectral structure reported here is similar to that observed when a water hammer is used to generate SL [14]. We note that emission lines are not apparent in the 4 torr bubble. A possible explanation [29] for this effect lies in a comparison of the energy flux densities of the 4 and 50 torr SA bubbles. Although SL from the 50 torr bubble is ~100 times more energetic than the 4 torr bubble, its energy flux density is smaller. From this perspective, processes that lead to the SL spectral continuum are hotter than the processes that excite various species.

The bright 50 torr Xe in aqueous SA bubbles is in equilibrium with respect to mass diffusion. An estimate [30] of the gas concentration "C_∞" that maintains equilibrium with a pulsating bubble is $C_\infty/C_0 \sim 3[R_0/R_m]^3$, where C_0 is the concentration of gas under an ambient pressure head of 1 atm. For the observed bubble radii, one calculates $C_\infty \sim 50$ torr in agreement with the experimental preparation. It should be noted that according to measured parameters the 50 torr Xe-water bubbles would be in equilibrium with an 8 torr mixture. In this case, unbalanced mass diffusion leads to a pinch-off instability [31].

The question remains: Why is it possible to achieve light emission from Xe bubbles in SA that are 1500 times brighter [12] than the room temperature bubbles in water? According to an analysis of the 4 torr Xe in SA and water bubbles of Fig. 2, a factor of 10 could reasonably be ascribed purely to the lower vapor pressure of SA. At xenon pressures of 4 torr dissolved into the liquid, changing fluid parameters from water at room temperature to water at 1 °C lowers the vapor pressure from 20 to 5 torr with a factor of 10 increase in light intensity. Changing fluid parameters from water at 1 °C to SA lowers the vapor pressure by a factor of 100 but with no corresponding increase in light intensity. Of course, in experimental sonoluminescence it is very difficult to change just one parameter: the water system has a slightly larger R_0 and a much lower viscosity. Also, in changing fluids, the chemical composition inside the bubble has changed, which changes both the potential emitting species and the endothermic chemical reactions during bubble collapse.

A new and surprising effect occurs as the partial pressure of xenon is increased to 50 torr at constant vapor pressure of the SA. Although the bubble's ambient radius increases by about a factor of 3, its implosion becomes remarkably weaker; the expansion ratio drops from 7.5 to 3.5 and the calculated Rayleigh-Plesset collapse velocity goes down by a factor of 5. Furthermore, the van der Waals excluded volume of the collapsed bubble is only 25% of the total volume, so that deviations from the ideal gas equation of state are, for SL, relatively small. Yet these bubbles develop a strongly emitting surface whose radius is nearly equal to R_c.

Sonoluminescence from bubbles in sulfuric acid exposes a new region of parameter space where light emission can be up to 100 times greater than is observed with cold water. This increase is correlated with the appearance of rapid translational motion of the bubble. Evidence for energy focusing nonlinear processes within the bubble is provided by the observation that the implosion velocity must exceed a sharp threshold in order for a flash to be emitted. Imposition of a restriction that the radius of the emitting hot spot is smaller than the radius of the gas bubble has been shown to imply the presence of a surface emitting blackbody which masks the, as yet, unmeasured core temperature of sonoluminescence.

We acknowledge valuable discussions with Avik Chakravarty and David Flannigan. This research was supported by DARPA and by NSF (CHE0315494).

[1] B. P. Barber and S. J. Putterman, Nature (London) **352**, 318 (1991).
[2] G. E. Vazquez *et al.*, Opt. Lett. **26**, 575 (2001).
[3] C. Camara, S. Putterman, and E. Kirilov, Phys. Rev. Lett. **92**, 124301 (2004).
[4] W. C. Moss *et al.*, Phys. Rev. E **59**, 2986 (1999).
[5] A. J. Walton and G. T. Reynolds, Adv. Phys. **33**, 595 (1984).
[6] G. E. Vazquez and S. J. Putterman, Phys. Rev. Lett. **85**, 3037 (2000).
[7] H. Kutruff, Acustica **12**, 230 (1962).
[8] K. S. Suslick, J. W. Goodale, H. H. Wang, and P. F. Schubert, J. Am. Chem. Soc. **105**, 5781 (1983).
[9] M. P. Brenner, S. Hilgenfeldt, and D. Lohse, Rev. Mod. Phys. **74**, 425 (2002).
[10] Y. T. Didenko and K. S. Suslick, Nature (London) **418**, 394 (2002).
[11] A. Troia, D. Madonna Ripa, and R. Spagnolo, *World Congress of Ultrasonics 2003*, edited by D. Cassereau (Societe Francaise d'Acoustique, Paris, 2003), pp. 1041–1044.
[12] D. J. Flannigan and K. S. Suslick, Nature (London) **434**, 52 (2005).
[13] C. K. Su *et al.*, Phys. Fluids **15**, 1457 (2003).
[14] A. Chakravarty *et al.*, Phys. Rev. E **69**, 066317 (2004).
[15] B. P. Barber, R. Hiller, R. Löfstedt, S. J. Putterman, and K. R. Weninger, Phys. Rep. **281**, 65 (1997).
[16] R. Hickling, J. Acoust. Soc. Am. **35**, 967 (1963).
[17] A. Prosperetti, J. Fluid Mech. **222**, 587 (1991).
[18] Y. T. Didenko, W. B. McNamara III, and K. S. Suslick, Nature (London) **407**, 877 (2000).
[19] K. R. Weninger *et al.*, J. Phys. Chem. **99**, 14 195 (1995).
[20] C. C. Wu and P. H. Roberts, Phys. Rev. Lett. **70**, 3424 (1993).
[21] R. Löfstedt, B. P. Barber, and S. J. Putterman, Phys. Fluids A **5**, 2911 (1993).
[22] H. P. Greenspan and A. Nadim, Phys. Fluids A **5**, 1065 (1993).
[23] S. J. Putterman, P. G. Evans, G. Vazquez, and K. Weninger, Nature (London) **409**, 782 (2001).
[24] Ya. B. Zeldovich and Yu. P. Raizer, *Physics of Shock Waves and High Temperature Hydrodynamic Phenomena* (Academic, New York, 1966).
[25] F. Reif, *Fundamentals of Statistical and Thermal Physics* (McGraw-Hill, Boston, 1965).
[26] K. S. Suslick *et al.*, Phil. Trans. R. Soc. A **357**, 335 (1999); W. B. McNamara, Y. T. Didenko, and K. S. Suslick, Nature (London) **401**, 772 (1999); E. B. Flint and K. S. Suslick, Science **253**, 1397 (1991).
[27] J. B. Young, J. A. Nelson, and W. Kang, Phys. Rev. Lett. **86**, 2673 (2001).
[28] K. R. Weninger, C. G. Camara, and S. J. Putterman, Phys. Rev. E **63**, 016310 (2001).
[29] Avik Chakravarty (private communication).
[30] R. Löfstedt *et al.*, Phys. Rev. E **51**, 4400 (1995).
[31] B. P. Barber *et al.*, Phys. Rev. Lett. **74**, 5276 (1995).